Contents lists available at ScienceDirect

Physics Letters B

The (6$^+$) isomer in ^{102}Sn revisited: Neutron and proton effective charges close to the double shell closure

H. Grawe [a,1], K. Straub [b], T. Faestermann [b,*], M. Górska [a], C. Hinke [b], R. Krücken [b],
F. Nowacki [c], M. Böhmer [b], P. Boutachkov [a], H. Geissel [a], R. Gernhäuser [b], A. Gottardo [d],
J. Grębosz [e], N. Kurz [a], Z. Liu [d], L. Maier [b], S. Pietri [a], Zs. Podolyák [f], K. Steiger [b], H. Weick [a],
H.J. Wollersheim [a], P.J. Woods [d], N. Al-Dahan [f,g], N. Alkhomashi [f], A. Ataç [h,i], A. Blazhev [j],
N. Braun [j], I. Čeliković [k], T. Davinson [d], I. Dillmann [b], C. Domingo-Pardo [a], P. Doornenbal [a],
G. Farrelly [f], F. Farinon [a], G. de France [l], J. Gerl [a], N. Goel [a], T. Habermann [a], R. Hoischen [a],
R. Janik [m], M. Karny [n], A. Kaşkaş [h], I. Kojouharov [a], Th. Kröll [b], M. Lewitowicz [l],
Yu.A. Litvinov [a], S. Myalski [e], F. Nebel [b], S. Nishimura [o], C. Nociforo [a], J. Nyberg [p], A. Parikh [b],
A. Procházka [a], P.H. Regan [f,q], C. Rigollet [r], H. Schaffner [a], C. Scheidenberger [a], S. Schwertel [b],
P.-A. Söderström [p], S. Steer [f], A. Stolz [s], P. Strmeň [m], and the RISING Collaboration

[a] *GSI Helmholtzzentrum für Schwerionenforschung GmbH, D-64291 Darmstadt, Germany*
[b] *Physics Department E12, Technical University of Munich, D-85748 Garching, Germany*
[c] *Université de Strasbourg, CNRS, IPHC UMR 7178, F-67000 Srasbourg, France*
[d] *School of Physics and Astronomy, The University of Edinburgh, Edinburgh, EH9 3FD, UK*
[e] *The Henryk Niewodniczanski Institute of Nuclear Physics (IFJ PAN), 31-342 Krakow, Poland*
[f] *Department of Physics, University of Surrey, Guildford GU2 7XH, UK*
[g] *Faculty of Dentistry, University of Alkafeel, Najaf, Iraq*
[h] *Physics Department, Faculty of Science, Ankara University, 06100 Tandogan, Ankara, Turkey*
[i] *Department of Physics, Royal Institute of Technology (KTH), SE-10691 Stockholm, Sweden*
[j] *Institute of Nuclear Physics, University of Cologne, D-50937 Cologne, Germany*
[k] *Institute Vinca, University of Belgrade, 11000 Belgrade, Serbia*
[l] *Grand Accélérateur National d'Ions Lourds, CEA/DSM-CNRS/IN2P3, 14076 Caen, France*
[m] *Comenius University, 81806 Bratislava 16, Slovakia*
[n] *Faculty of Physics, University of Warsaw, PL-02093 Warsaw, Poland*
[o] *RIKEN Nishina Center, Wako, Saitama 351-0198, Japan*
[p] *Department of Physics & Astronomy, Uppsala University, SE-75120 Uppsala, Sweden*
[q] *National Physical Laboratory, Teddington, Middlesex TW11 0LW, UK*
[r] *KVI, University of Groningen, 9747AA Groningen, the Netherlands*
[s] *National Superconducting Cyclotron Laboratory, Michigan State University, East Lansing, MI 48824-1321, USA*

ARTICLE INFO

ABSTRACT

In a high-energy fragmentation experiment at GSI an $I^\pi = (6^+)$ isomer and its γ-decay are identified in ^{102}Sn, the two-neutron neighbour of the doubly-magic ^{100}Sn. Its half-life is measured to be $T_{1/2} = 367(11)$ ns. The possible existence of further isomers is discussed in the framework of large-scale shell model (LSSM) calculations including up to five particle-hole excitations of the ^{100}Sn core. From the precise B(E2; $6^+ \rightarrow 4^+$) strength and the recently remeasured value for B(E2; $8^+ \rightarrow 6^+$) in the two-proton hole neighbour ^{98}Cd effective E2 polarization charges for protons and neutrons were inferred including LSSM corrections within the full N=4 $0\hbar\omega$ space. The results are discussed in comparison to predicted and empirically determined effective operators.

1. Introduction

The doubly-magic ^{100}Sn, the heaviest N=Z nucleus stable against nucleon emission, and its neighbours were subject of nu-

* Corresponding author.
E-mail address: thomas.faestermann@tum.de (T. Faestermann).
[1] Deceased: 8 November 2020.

merous experimental and theoretical nuclear-structure studies. The main research topics were single-particle (hole) energies, shell gaps and stability with respect to core-excitation, super-allowed Gamow-Teller and γ-decay, proton emission and quadrupole response investigated with state-of-the-art experimental techniques, as summarised in a recent review [1]. Effective E2 charges have been studied systematically in N, Z $\leq$ 50 nuclei [2] and more recently in the Sn isotopic chain [3]. Common, constant, orbit specific [4] and isospin dependent [5] polarization charges have been employed in these studies. The isovector effects exhibited in polarisation charge values in the ^{100}Sn region can be discussed in comparison with the region of the lighter N=Z doubly magic nucleus ^{56}Ni where also the single-particle spin-orbit partners are placed on the opposite side of the shell gap (LS-open core). The latter region was addressed in the literature [6,7]. The empirical extraction of effective operators requires precise lifetime determination of states with high configurational purity to separate configuration space dependent and higher-order (from $2\hbar\omega$ excitation) contributions. Therefore, isomers in the two-neutron particle Z=50 isotope ^{102}Sn and the two-proton hole N=50 isotone ^{98}Cd provide excellent probes to study the effective E2 operator around ^{100}Sn in detail. The level schemes have been established in ^{98}Cd [8–10] and ^{102}Sn [11,12] and lifetimes with limited accuracy were extracted for the respective isomers. Recently, a more accurate value was determined for the $I^\pi = (8^+)$ isomer in ^{98}Cd [13] leaving the ^{102}Sn $I^\pi = (6^+)$ state to be re-investigated.

2. Experimental details

The "^{100}Sn experiment" [14] was performed at the Fragment Separator (FRS) of the GSI Helmholtzzentrum für Schwerionenforschung, Darmstadt. More details can be found in the PhD theses [15,16]. A beam of ^{124}Xe was accelerated with the GSI accelerators UNILAC and SIS18 to an energy of 1.0 A GeV and irradiated a beryllium target with a thickness of 4.0 g/cm^2. The synchrotron ejected a spill every 3 s for a period of 1 s. The average beam intensity was about 10^9 ions/s.

The fragments produced in the target were separated in the FRS by a combination of four magnetic deflections and energy losses in aluminium degraders of thickness 2.0 g/cm^2 in the first focal plane F1 and a wedge-shaped degrader with an average thickness of 4.5 g/cm^2 in the second focal plane F2. The fragments were identified between F2 and the final focus F4 by measuring their time of flight, their position at F2 and F4, their angle at F4 and their energy loss in multiple sampling ionization chambers at F4. Thus, a mass resolution of $\delta A \approx 0.30$ (FWHM) and a nuclear charge resolution of $\delta Z \approx 0.23$ (FWHM) were achieved. After the degrader at F2 the fragments still had about 500 A MeV and 98% of the ions were completely stripped off bound electrons. Assuming bare nuclei on the proton rich side did not pose a problem, since one could only mistake a Z=Q+1 for a Z=Q nucleus, and background could only come from more exotic nuclides that have a much smaller production rate.

After being identified the ions of interest passed another degrader to be stopped in the implantation detector, a stack of three highly segmented Si detectors [14], that serve for β, proton, and α spectrometry. However, only the implantation signal was used in the present context. The total flight time of the ions through the FRS amounts to 200(5) ns in their own rest frame. The implantation detectors were mounted in the centre of the "stopped beam" RISING array. This is an assembly of 15 Euroball cluster detectors with seven Ge-crystals each, arranged in three rings around the beam axis. A detailed description is given by Pietri et al. [17]. The γ-ray efficiencies are modified due to absorption and scattering in the implantation detector and its electronics. They have been determined by GEANT4 simulations as well as experimen-
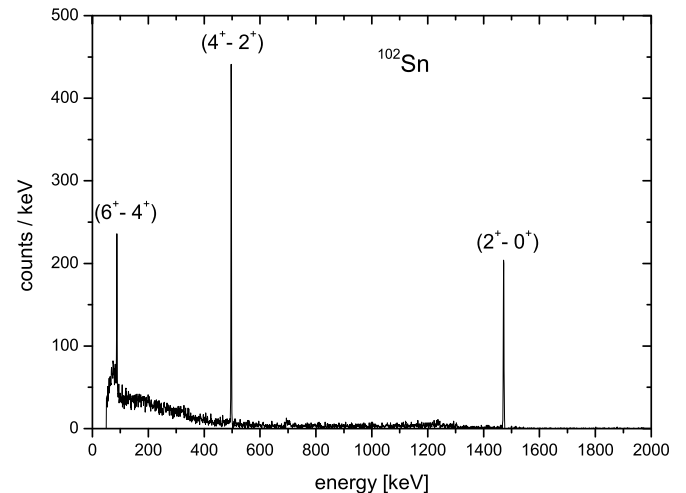

Fig. 1. Delayed (0.25 µs to 6 µs) γ-spectrum for identified ^{102}Sn nuclei. The lines at 1471.7 keV, 496.9 keV and 87.6 keV are labelled with the tentative assignments for the transitions $2^+ \rightarrow 0^+$, $4^+ \rightarrow 2^+$, and $6^+ \rightarrow 4^+$, respectively.

tally with standard γ-ray sources and with isomeric decays produced in-beam [15,16]. In addback-mode the photo-peak efficiency amounts to 10% at 1.33 MeV. The last scintillation detector before the implantation detector provided the trigger signal that started the digital readout of the γ-information.

3. Results and discussion

3.1. Isomer assignment and level scheme

Although the FRS was set for ^{100}Sn fragments, about 50,000 ^{102}Sn nuclei were identified and implanted in the 15-day long experiment. The delayed (between 0.25 and 6 µs after implantation) γ-spectrum from identified ^{102}Sn nuclei is shown in Fig. 1. We clearly see the known [11,12] lines at 1471.7(3) keV and at 496.9(3) keV, that were interpreted as the $2^+ \rightarrow 0^+$ and $4^+ \rightarrow 2^+$ transitions, respectively, fed by the decay of a 6^+ isomer. In addition, a low-energy line is seen at 87.6(3) keV that had not been observed before. Since the centroid of the ^{102}Sn fragment distribution is displaced by about 50 mm from the centre, a major part of them is stopped at an ill-defined position and thus the γ-efficiency is not well known. But using the calculated efficiencies for a source in the centre of the implantation detector and E2-conversion for the 87.6 keV line [18,19], the three lines 87.6 keV: 496.9 keV: 1471.7 keV have intensity ratios of 1.30(30): 1.05(3): 1.00(4). From the absolute intensity we can deduce that even 250 ns after the implantation 25% of the ^{102}Sn fragments are in the isomeric state. All three lines are mutually in coincidence, *i.e.* they form a cascade. If we assumed M1 multipolarity for the 87.6 keV transition, its intensity ratio to the 1472 keV transition would be 0.67(15), making the assumption of an E2 character more probable. Therefore, the natural assignment is the $6^+ \rightarrow 4^+$ transition for the 87.6 keV line and thus the transition depopulating the isomer. The time distributions of the three transitions 87.6, 496.9, 1471.7 keV show consistent half-lives with 392(29) ns, 366(10) ns and 362(13) ns, resulting in a combined half-life of 367(11) ns, where a systematic uncertainty of 7 ns due to the choice of the starting time of the fit has been added in quadrature. This is the value for the isomer that we quote. The sum of the time distributions for the 496.9 keV and 1471.7 keV lines is shown in Fig. 2. It is fitted with a half-life of 366(9) ns. For the fitting the maximum likelihood method was used, that takes the Poisson distribution of the events in the histogram properly into account. The fitted background is compatible with zero: 0.004(17). The newly obtained
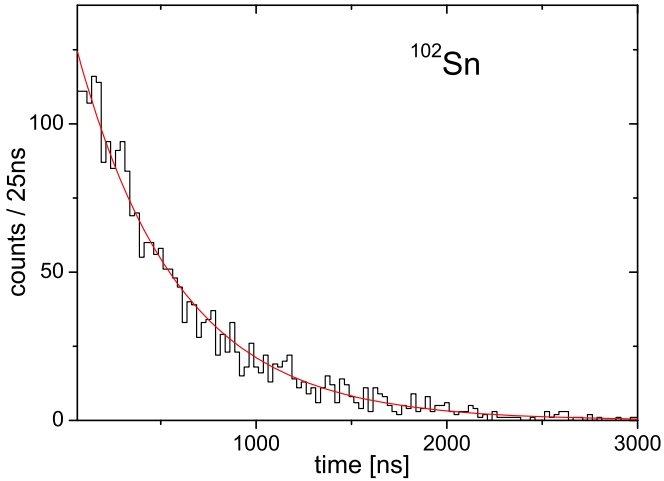
Fig. 2. Time distribution for the sum of the 496.9 keV and 1471.7 keV γ-ray lines observed after stopping ^{102}Sn fragments. The time scale starts about 100 ns after implantation. The line through the histogram represents the result of the maximum-likelihood fit yielding $T_{1/2} = 366(9)$ ns.

half-life value is within 1.3 σ compatible with the previous values 1.0(5) μs [11] and $(0.62^{+0.43}_{-0.19})$ μs [12]. The weighted average of our and the two previous values [11,12] is 368(11) ns with a $\chi^2 = 3.4$ and two degrees of freedom corresponding to a p-value of 0.19. From our half-life value and the theoretical conversion coefficient $\alpha = 2.55(4)$ [18,19], we deduce a transition strength of B(E2) = 84.2(31) $e^2 fm^4$ = 2.97(11) W.u. (Weisskopf or single-particle units), where uncertainties from $T_{1/2}$, α and E_γ are included.

Disturbing is the fact that, in an effort to search for the isomeric $6^+ \rightarrow 4^+$ transition, Lipoglavšek et al. [12] had observed a 44 keV conversion electron line in coincidence with the sum of the 497 keV and 1472 keV γ-transitions and attributed this tentatively to a highly L-converted 48 keV transition. In principle, two different isomeric states, 40 keV apart, could be populated and observed in fusion-evaporation reactions [11,12] and in the present fragmentation reaction. In addition, both from the balance of the delayed γ-intensities as from the perfect fit of the $(4^+ \rightarrow 2^+)$ and $(2^+ \rightarrow 0^+)$ γ-ray time spectra with a single half-life we can exclude a more than 20% feeding of the (4^+) state from an unobserved isomer. Thus, we assume that the 87.6 keV transition is depopulating the lowest 6^+ state in ^{102}Sn and it is not sure whether this transition could have been observed in the two previous experiments [11,12], because of the probability for γ-emission of only 28% and an estimated threshold of the γ-detectors of about 80 keV [20]. The discrepancy will be further discussed in Sec. 3.3.

3.2. Shell-model calculations

To elucidate the isomer puzzle and to investigate structural reasons for possible isomerism, three sets of shell-model calculations have been performed in different model spaces employing nucleon-nucleon (NN) interactions based on free NN potentials such as Paris [21] and CD-Bonn [22] with renormalisation of the G-matrix [23]. Two-body matrix elements (TBME) were monopole tuned to reproduce extrapolated single-particle (hole) energies in ^{100}Sn [1]. For the Sn chain in the simplest approach a pure neutron valence space was used with TBME from a realistic interaction derived for a ^{88}Sr core in a $\pi(p_{1/2}, g_{9/2})$, $\nu(g_{7/2}, d, s, h_{11/2})$ model space (MHJM) [24] and recently applied in the Cd chain [25,26]. Including excitations of the ^{100}Sn core requires an extended model space, which was chosen to be the full proton-neutron $\pi\nu(g, d, s)$ space and employed the CD-Bonn based G-matrix renormalized

SDGN interaction [9,27]. This interaction in a large-scale shell-model (LSSM) approach with up to five particles and five holes (5p5h; t=5) excited across the N=Z=50 double shell closure has been proven to give an excellent description of isomer structure, electromagnetic and β^+/EC transition strength for even-parity states in ^{100}Sn and its neighbours [14,28–32].

To investigate odd-parity isomerism in a third approach the $\nu h_{11/2}$ orbit was implemented in the $\pi\nu(g, d, s)$ model space to create an active $\pi(g, d, s)$, $\nu(g, d, s, h_{11/2})$ space. The SNET interaction from the OXBASH package [33] was employed, which for a ^{102}Sn calculation and the chosen truncation is identical with H7B [21]. Core excitation was restricted to 1p1h in the subspace $\pi\nu(g_{9/2} \rightarrow g_{7/2}, d_{5/2}, d_{3/2})$ (i.e. $t_\pi = t_\nu = 1$) plus $\nu(g_{9/2} \rightarrow h_{11/2})$ for odd-parity states. The results of the three shell-model approaches are compared to the experimental level scheme in Fig. 3 and found to be in good agreement with the known level structure.

3.3. The isomer puzzle

The shell-model levels shown in Fig. 3 may be grouped according to their leading configurations in well separated categories, namely two-neutron valence $\nu(g, d, s)^2$ even-parity and $\nu(g, d, s) \otimes h_{11/2}$ odd-parity, core excited and $\nu(h_{11/2})^2$ states. All groups may exhibit isomerism either within the group or for transitions between different configurations. For estimates of possible decay paths standard effective operators were used for E2 and M1 with polarization charge 0.5 e and effective g-factors $g_s = 0.7 g_s^{free}$ for both protons and neutrons. E1 and M2 reduced transition probabilities were assumed to have values typical for Sn and Cd neighbours [34]. These are B(M2) = 0.21 W.u. and B(E1) = 1.8×10^{-5} W.u. within about a 5% variation.

From the valence $\nu(g_{7/2}, d, s)$ orbitals available in the major neutron shell $50 \leq N \leq 82$, one expects exactly two low-lying 6^+ states, dominated by the coupling of $\nu(d_{5/2}, g_{7/2})$ and $\nu(g_{7/2})^2$ neutron configurations. Earlier shell-model calculations, however, predicted these to be 700-800 keV apart [35,36]. Both calculations have the $d_{5/2}$ single particle energy 200 keV below the $g_{7/2}$. But even inverting these two levels, as suggested from the ^{105}Te α-decay feeding levels in ^{101}Sn [37], would lower the spacing between the 6^+ states only to about 400 keV. The results from the present work, shown in Fig. 3, yield $6_2^+ \rightarrow 6_1^+$ distances of 850 - 1000 keV. In all cases, calculated E2 and M1 strengths fail to support a second isomer due to the large γ-decay energy, even though a pure $\nu(g_{7/2})^2 \rightarrow \nu(d_{5/2}, g_{7/2})$ M1 transition would be ℓ - forbidden.

The option of a $\nu(h_{11/2})^2$; $I^\pi = 10^+$ isomer may be discarded as these states are above the yrast line by a large margin in energy. The state which has this dominant configuration is the 10^+ state calculated at 8.6 MeV (SNET in Fig. 3). Notably, it is the eighth 10^+ state.

Below the shell gap at particle number 50, core excited $\Delta I = 4$ spin-gap isomers are known in the neighbouring ^{98}Cd [9,10] and ^{96}Ag [28] to feed the maximum-spin $(g_{9/2})^{-n} I^\pi = 8^+$ and 15^+ isomers, respectively. In ^{102}Sn $I^\pi = 10^+$ would be the corresponding candidate decaying by a low-energy E2 to $I^\pi = 8^+$, which is energetically clearly not supported by the shell-model calculation. Also, in the SDGN approach B(E2) strengths are calculated to have several W.u. Moreover, the intermediate 9^+ would enable even faster M1 transitions. Similarly, existence of an $I^\pi = 12^+$ isomer, analogue to the observed E6 isomers in ^{96,97}Cd [29] [34] and predicted to be yrast in ^{98}Cd as $I^\pi = 14^+$ [9], can be excluded due to the predicted E2 decay energy. In addition, γ-rays possibly bypassing the 6_1^+ state should be observed, at variance with the spectrum shown in Fig. 1. The reason for the missing spin-trap character in ^{102}Sn is the different ph structure and overlap. In
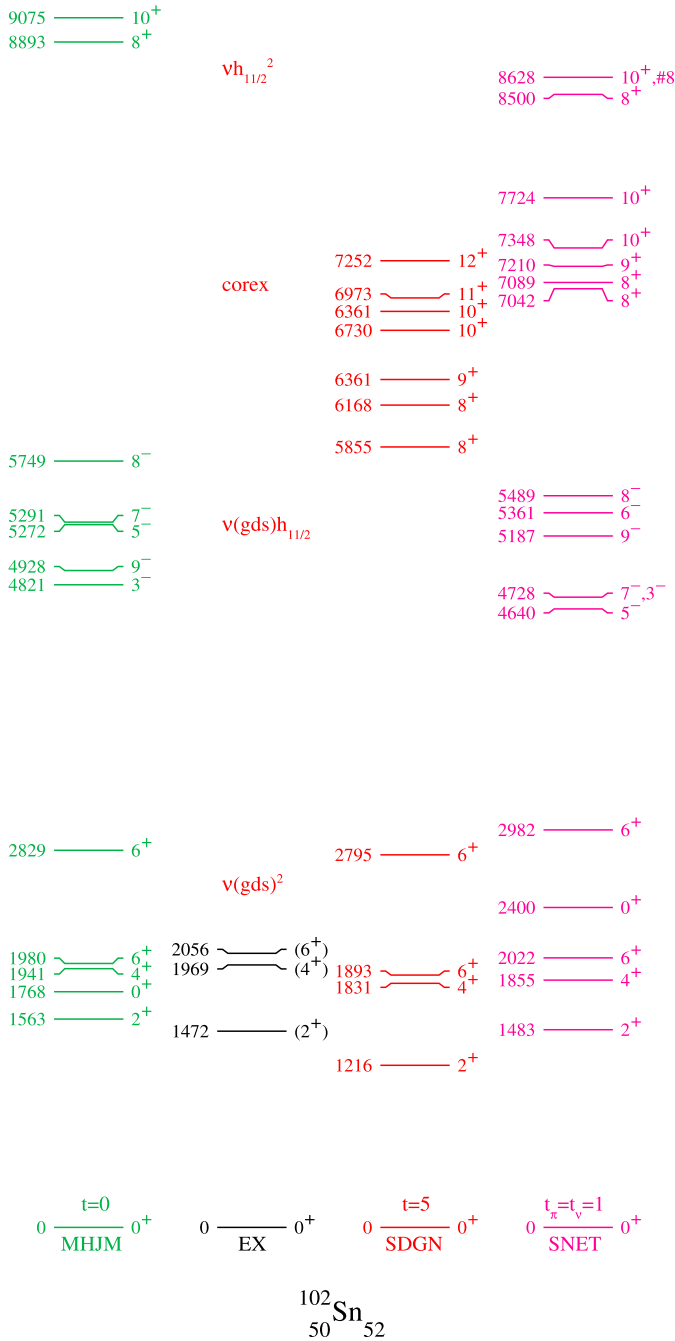
Fig. 3. ^{102}Sn experimental and shell-model level schemes for pure valence space $\nu(g_{7/2}, d, s, h_{11/2})$ (MHJM), inclusion of core excitation ("corex") in $\pi\nu(g, d, s)$ (SDGN) at t=5, and $\pi(g, d, s)$, $\nu(g, d, s, h_{11/2})$ at $t_\pi = t_\nu = 1$ (SNET). The eighth 10^+ state at 8.6 MeV for SNET has the dominant $\nu(h_{11/2})^2$ configuration. See text for details.

^{98}Cd the dominating 3h1p $\pi(g_{9/2})^{-2} \otimes \nu(g_{9/2}^{-1}d_{5/2})$ configuration couples the $I^\pi = 25/2^+$ prolate E6 spin trap in ^{97}Cd [34] non-stretched to a $\nu d_{5/2}$ particle to maintain maximal spatial overlap. In ^{102}Sn, on the other hand, the analogue configuration would be 3p1h $\nu(d_{5/2}, g_{7/2})^2 \otimes \pi(g_{9/2}^{-1}d_{5/2})$, i.e. a hypothetical $I^\pi = 17/2^+$ oblate E2 isomer in ^{103}Sb would couple to a non-aligned $\pi g_{9/2}$ hole for the same overlap reason giving rise to non-isomeric 8^+ states due to the large decay energy to $6^+_{1,2}$ (see Fig. 3). A sequential $\gamma - p - \gamma$ decay via the shell-model predicted E2 isomer in ^{103}Sb; $17/2^+ \to \gamma \to 13/2^+ \to p \to {}^{102}$Sn; 4^+ is excluded by the experimental conditions set in Refs. [11,12].

Odd-parity states with leading configuration $\nu(g_{7/2}, s, d, h_{11/2})$ may produce both $I^\pi = 9^-$ E3 and $I^\pi = 7^-$ E2 isomers (see Fig. 3). In both cases long-lived isomers are unlikely. E3 transitions of $\approx$ 2.5 MeV and enhanced E3 strength due to the stretched $h_{11/2} \to d_{5/2}$ conversion are known in the neighbouring ^{104}Sn with $T_{1/2} \approx$ 50 ps [38] and well reproduced in shell-model calculations. In summary, the existence of a second isomer appears to be unlikely at the present state of shell-model and experimental evidence.

However, there may be an experimental solution to the apparent discrepancy on the isomeric $6^+ \to 4^+$ transition energy based on an alternative interpretation of the Lipoglavšek et al. [12] data. The isomeric 87.6 keV γ-transition, reported in the present work, is in competition with 58.4 keV conversion electrons because of a K-conversion coefficient of $\alpha_K(E2) = 1.77$ [19]. Each filled K-hole would be accompanied by Sn x-rays (or Auger electrons). Indeed, in the spectrum of Lipoglavšek et al. [12] a line close to 25.3 keV is visible, the Sn K_α energy. But the electron line is observed at 44 keV, 14 keV lower than expected for a K-converted 87.6 keV transition. Unfortunately, in Ref. [12] nothing is mentioned if and how energy loss of the electrons between source and detector has been taken into account, and it seems that the original notes from the experiment cannot be recovered anymore [20]. In that experiment the recoil nuclei were stopped in a 4.2 mg/cm^2 Al foil from which decay radiation had to emerge towards the detectors. Only 3 mg/cm^2 are needed to slow electrons down from 58 keV to 44 keV [39]. A range distribution of the recoil nuclei with an assumed width of 1 mg/cm^2 would contribute about 5 keV to the width of the electron energy distribution. Although the line observed [12] seems narrower than the typical resolution of 6 keV, a combined width of 8 keV might still be possible for the observed 7 events. For 7 coincident electrons from K-conversion [12] we would expect 2.5 electrons from L-conversion, emitted with 83 keV and detected after a 30% smaller energy loss with about 73 keV. Although no electron was observed in the energy range between 70 keV and 85 keV, the Poisson distribution for 2.5 expected events leaves an 8% chance to observe not a single one. So, there are explanations that both experiments have observed the 87.6 keV transition, and hence the same isomer.

3.4. Effective proton and neutron E2 charge extracted from ^{102}Sn and ^{98}Cd

To determine effective proton and neutron E2 charges close to ^{100}Sn we have chosen the $I^\pi = (6^+)$ and the $I^\pi = (8^+)$ isomers in ^{102}Sn and ^{98}Cd, respectively. The former was established in the present work while the latter has been remeasured more precisely in a EURICA experiment at RIKEN [13]. In the analysis the shell-model approach SDGN, as described in Sec. 3.2 and shown in Fig. 3, was used as it includes core excitation across Z, N = 50 in the full $\pi\nu(g, d, s)$ model space. Truncation level t=5 was chosen for both ^{98}Cd and ^{102}Sn. This approach accounts for the $0\hbar\omega$ contributions to the effective operator and allows to extract the $2\hbar\omega$ part which may be compared to theoretical predictions [4,5]. Thus, besides the leading proton (^{98}Cd) and neutron (^{102}Sn) minimum valence space contribution the core excited part of the E2 matrix element is considered explicitly. In the wave functions of the isomers the t=0 content is $\approx$ 76% for both nuclei. The B(E2) value may be decomposed in its proton (π) and neutron (ν) matrix elements as B(E2; $I_i \to I_f$) = $(2I_i + 1)^{-1} |e_\pi M_\pi + e_\nu M_\nu|^2$ with M taken from shell-model calculations and the effective charges e_π and e_ν treated as variables. The input values are listed in Table 1. For comparison the values for t = 0 for both ^{98}Cd and ^{102}Sn using the MHJM interaction, are given too. The results are listed in Table 2 and compared with theoretical predictions and empirical fits in several adjacent model spaces.

Table 1

Input data for the extraction of the effective E2 charges. For comparison B(E2) values were calculated using standard effective charges $e_\pi = 1.5e$ and $e_\nu = 0.5e$; M_π and M_ν are the corresponding proton and neutron matrix elements. See text for details.

$I_i^\pi \rightarrow I_f^\pi$ nucleus	B(E2) $[e^2 fm^4]$ Exp	B(E2) $[e^2 fm^4]$ Standard	t	M_π(E2) $[efm^2]$	M_ν(E2) $[efm^2]$
$6^+ \rightarrow 4^+$	84.2(31)	55.24	5	8.51	28.06
^{102}Sn	this work	10.72	0	-	23.61
$8^+ \rightarrow 6^+$	38.6(44)	56.89	5	18.89	5.52
^{98}Cd	[13]	38.87	0	17.14	-

Table 2

Empirical and predicted effective E2 charges in the ^{100}Sn region. For the t=5 calculation the SDGN interaction has been used and for the t=0 calculation the MHJM interaction. For comparison, the effective charges in the ^{56}Ni region are shown too.

e_π/e	e_ν/e	Model space	t	Ref.
1.11(7)	0.84(2)	$\pi\nu(g,d,s)$	5	this work
1.49(8)	1.40(3)	$\pi(p_{1/2}, g_{9/2})\nu(g_{7/2}, d, s, h_{11/2})$	0	this work
1.18	0.82	N=Z		[5]
1.35	-	$\pi(f_{5/2}, p, g_{9/2})$, N=50		[4]
-	1.44	$\nu(g_{7/2}, d, s, h_{11/2})$, Z=50		[35]
~ 1.15	~ 0.80	$\pi\nu(f, p)$, N≈Z≈28	5	[6]

The extracted effective charges clearly exhibit the effect of an incomplete *versus* a full $0\hbar\omega$ model space which amounts to a correction of about 0.4e and 0.6e for protons and neutrons, respectively. This compares well with empirically fitted values in limited model spaces [2,25]. The results impressively demonstrate the iso-vector dependence of the effective E2 polarization charge introduced by Bohr and Mottelson [5] with almost quantitative agreement. Even more impressive is the fact of perfect consistency of those results with the values extracted in the region of ^{56}Ni [6] as shown in the last line of Table 2. These results are to be distinguished from LS-closed core ^{40}Ca [40]. The drastic reduction of the proton polarization charge, first invoked for ^{98}Cd without knowledge of core excited states [8] and inferred under improved experimental conditions [9,13,41], is firmly established in the present analysis. The neutron charge is unexpectedly large and the empirical rule for effective E2 charges $e_\pi + e_\nu \approx 2e$ [5,42] is confirmed. Coraggio et al. [4] have developed a method to calculate orbit-specific electromagnetic operators including core polarization effects. The average value for a $\pi(f_{5/2}, p, g_{9/2})$ space is listed in Table 2, intermediate between the still smaller model space $\pi(p_{1/2}, g_{9/2})$ and the full $0\hbar\omega$ $\pi\nu(g,d,s)$ space. For the Sn isotopes with $50 \leq N \leq 82$ Togashi et al. [43] have performed Monte Carlo Shell-Model calculations in an even larger model space and obtained good agreement for B(E2; $2^+ \rightarrow 0^+$) with constant small and large polarization charges for protons and neutrons, respectively. Nevertheless overpredictions towards ^{132}Sn seem to indicate an iso-vector dependence of the effective operator.

4. Summary

In summary, an $I^\pi = (6^+)$ isomer and its γ-decay are identified in ^{102}Sn. Although the energy of the isomeric transition seems different from one suggested earlier [12] there might have been a misinterpretation in that work. From its half-life and B(E2) and corresponding data in ^{98}Cd [13] effective polarization charges are determined including corrections in the full N=4 $0\hbar\omega$ space. LSSM calculations including up to 5p5h excitations across the Z=N=50 shell closure have been performed to investigate the truncation dependence of empirical effective charges and the possible existence of further isomers in ^{102}Sn. The universality of the isovector dependence of the effective E2 polarization charge introduced by Bohr and Mottelson [5] is underlined based on the comparison to the results in the ^{56}Ni region.

Declaration of competing interest

The authors declare that they have no known competing financial interests or personal relationships that could have appeared to influence the work reported in this paper.

Acknowledgements

References

[1] T. Faestermann, M. Górska, H. Grawe, The structure of ^{100}Sn and neighbouring nuclei, Prog. Part. Nucl. Phys. 69 (2013) 85–130, https://doi.org/10.1016/j.ppnp.2012.10.002.

[2] D. Rudolph, K. Lieb, H. Grawe, Multiparticle-hole states of high spin in N ≤ 50, A ≈ 90 nuclei: 4. Systematics of level energies and electromagnetic properties, Nucl. Phys. A 597 (2) (1996) 298–326, https://doi.org/10.1016/0375-9474(95)00469-6.

[3] T. Bäck, C. Qi, B. Cederwall, R. Liotta, F. Ghazi Moradi, A. Johnson, R. Wyss, R. Wadsworth, Transition probabilities near ^{100}Sn and the stability of the N, Z = 50 shell closure, Phys. Rev. C 87 (2013) 031306, https://doi.org/10.1103/PhysRevC.87.031306.

[4] L. Coraggio, A. Covello, A. Gargano, N. Itaco, T. Kuo, Realistic shell-model calculations for proton-rich N=50 isotones, J. Phys. G, Nucl. Part. Phys. 26 (11) (2000) 1697–1708, https://doi.org/10.1088/0954-3899/26/11/305.

[5] A. Bohr, B. Mottelson, Nuclear Structure, vol. 2, Benjamin, 1975.

[6] R. du Rietz, et al., Effective charges in the fp shell, Phys. Rev. Lett. 93 (2004) 222501, https://doi.org/10.1103/PhysRevLett.93.222501.

[7] D. Rudolph, et al., Isospin symmetry and proton decay: identification of the 10^+ isomer in ^{54}Ni, Phys. Rev. C 78 (2008) 021301, https://doi.org/10.1103/PhysRevC.78.021301.

[8] M. Górska, et al., $^{98}_{48}$Cd$_{50}$: the two-proton-hole spectrum in $^{100}_{50}$Sn$_{50}$, Phys. Rev. Lett. 79 (1997) 2415–2418, https://doi.org/10.1103/PhysRevLett.79.2415.

[9] A. Blazhev, et al., Observation of a core-excited $E4$ isomer in ^{98}Cd, Phys. Rev. C 69 (2004) 064304, https://doi.org/10.1103/PhysRevC.69.064304.

[10] A. Blazhev, et al., High-energy excited states in ^{98}Cd, J. Phys. Conf. Ser. 205 (2010) 012035, https://doi.org/10.1088/1742-6596/205/1/012035.

[11] M. Lipoglavšek, et al., In-beam study of ^{102}Sn, Z. Phys. A, Hadrons Nucl. 356 (1996) 239.

[12] M. Lipoglavšek, et al., E2 polarization charge in ^{102}Sn, Phys. Lett. B 440 (3) (1998) 246, https://doi.org/10.1016/S0370-2693(98)01178-2.

[13] J. Park, et al., Properties of γ-decaying isomers and isomeric ratios in the ^{100}Sn region, Phys. Rev. C 96 (2017) 044311, https://doi.org/10.1103/PhysRevC.96.044311; Erratum: Phys. Rev. C 103 (2021) 049910.

[14] C. Hinke, et al., Superallowed Gamow-Teller decay of the doubly magic nucleus ^{100}Sn, Nature 486 (7403) (2012) 341–345, https://doi.org/10.1038/nature11116 and supplementary information.

[15] C. Hinke, Spectroscopy of the doubly magic nucleus ^{100}Sn and its decay, Ph.D. thesis, Technische Universität München, München, Germany, 2010, https://mediatum.ub.tum.de/?id=982004.

[16] K. Straub, Zerfallseigenschaften von Nukliden in der Umgebung von ^{100}Sn, Dissertation, Technische Universität München, München, Germany, 2011, http://mediatum.ub.tum.de/?id=1006184.

[17] S. Pietri, et al., Recent results in fragmentation isomer spectroscopy with RISING, Nucl. Instrum. Methods Phys. Res., Sect. B, Beam Interact. Mater. Atoms 261 (1) (2007) 1079–1083, https://doi.org/10.1016/j.nimb.2007.04.219.

[18] T. Kibédi, T. Burrows, M. Trzhaskovskaya, P. Davidson, C. Nestor, Evaluation of theoretical conversion coefficients using BrIcc, Nucl. Instrum. Methods Phys. Res., Sect. A, Accel. Spectrom. Detect. Assoc. Equip. 589 (2) (2008) 202–229, https://doi.org/10.1016/j.nima.2008.02.051.

[19] Web calculator, http://www.nndc.bnl.gov/bricc/.

[20] M. Lipoglavšek, D. Seweryniak, 2021, private communications.

[21] A. Hosaka, K.-I. Kubo, H. Toki, G-matrix effective interaction with the Paris potential, Nucl. Phys. A 444 (1) (1985) 76–92, https://doi.org/10.1016/0375-9474(85)90292-1.

[22] R. Machleidt, High-precision, charge-dependent Bonn nucleon-nucleon potential, Phys. Rev. C 63 (2001) 024001, https://doi.org/10.1103/PhysRevC.63.024001.

[23] M. Hjorth-Jensen, T. Kuo, E. Osnes, Realistic effective interactions for nuclear systems, Phys. Rep. 261 (3) (1995) 125–270, https://doi.org/10.1016/0370-1573(95)00012-6.

[24] O. Kavatsyuk, et al., Beta decay of ^{101}Sn, Eur. Phys. J. A 31 (3) (2007) 319–325, https://doi.org/10.1140/epja/i2006-10217-3.

[25] D.T. Yordanov, et al., Spins and electromagnetic moments of $^{101-109}$Cd, Phys. Rev. C 98 (2018) 011303, https://doi.org/10.1103/PhysRevC.98.011303.

[26] B.J. Coombes, et al., Spectroscopy and excited-state g factors in weakly collective ^{111}Cd: confronting collective and microscopic models, Phys. Rev. C 100 (2019) 024322, https://doi.org/10.1103/PhysRevC.100.024322.

[27] H. Mach, et al., Ultrafast-timing lifetime measurements in ^{94}Ru and ^{96}Pd: breakdown of the seniority scheme in N=50 isotones, Phys. Rev. C 95 (2017) 014313, https://doi.org/10.1103/PhysRevC.95.014313.

[28] P. Boutachkov, et al., High-spin isomers in ^{96}Ag: excitations across the Z=38 and Z=50, N=50 closed shells, Phys. Rev. C 84 (2011) 044311, https://doi.org/10.1103/PhysRevC.84.044311.

[29] B.S. Nara Singh, et al., 16$^+$ spin-gap isomer in ^{96}Cd, Phys. Rev. Lett. 107 (2011) 172502, https://doi.org/10.1103/PhysRevLett.107.172502.

[30] G. Guastalla, et al., Coulomb excitation of ^{104}Sn and the strength of the ^{100}Sn shell closure, Phys. Rev. Lett. 110 (2013) 172501, https://doi.org/10.1103/PhysRevLett.110.172501.

[31] P. Davies, et al., The role of core excitations in the structure and decay of the 16$^+$ spin-gap isomer in ^{96}Cd, Phys. Lett. B 767 (2017) 474–479, https://doi.org/10.1016/j.physletb.2017.02.013.

[32] P. Davies, et al., Toward the limit of nuclear binding on the N=Z line: spectroscopy of ^{96}Cd, Phys. Rev. C 99 (2019) 021302, https://doi.org/10.1103/PhysRevC.99.021302.

[33] B.A. Brown, OXBASH for Windows PC, MSU-NSCL report 1289, 2004.

[34] National Nuclear Data Center, Xundl: experimental unevaluated nuclear data list search and retrieval, https://www.nndc.bnl.gov/ensdf/XundlFetchServlet?, 2021.

[35] F. Andreozzi, L. Coraggio, A. Covello, A. Gargano, T.T.S. Kuo, Z.B. Li, A. Porrino, Realistic shell-model calculations for neutron deficient Sn isotopes, Phys. Rev. C 54 (1996) 1636–1640, https://doi.org/10.1103/PhysRevC.54.1636.

[36] H. Grawe, et al., High lights of modern nuclear structure, in: A. Covello (Ed.), Proc. 6th Int. Spring Seminar on Nucl. Phys., World Scientific, Singapore, 1999.

[37] I.G. Darby, et al., Orbital dependent nucleonic pairing in the lightest known isotopes of tin, Phys. Rev. Lett. 105 (2010) 162502, https://doi.org/10.1103/PhysRevLett.105.162502.

[38] M. Górska, et al., Structure of high spin states in ^{104}Sn: E2 and E3 polarization of the ^{100}Sn core, Phys. Rev. C 58 (1998) 108–115, https://doi.org/10.1103/PhysRevC.58.108.

[39] ESTAR calculator of NIST, https://physics.nist.gov/PhysRefData/Star/Text/ESTAR.html.

[40] R. Hoischen, et al., Isomeric mirror states as probes for effective charges in the lower pf shell, J. Phys. G, Nucl. Part. Phys. 38 (3) (2011) 035104, https://doi.org/10.1088/0954-3899/38/3/035104.

[41] J. Park, et al., Spectroscopy of ^{99}Cd and ^{101}In from β decays of ^{99}In and ^{101}Sn, Phys. Rev. C 102 (2020) 014304, https://doi.org/10.1103/PhysRevC.102.014304.

[42] M. Dufour, A. Zuker, Realistic collective nuclear Hamiltonian, Phys. Rev. C 54 (1996) 1641–1660, https://doi.org/10.1103/PhysRevC.54.1641.

[43] T. Togashi, Y. Tsunoda, T. Otsuka, N. Shimizu, M. Honma, Novel shape evolution in Sn isotopes from magic numbers 50 to 82, Phys. Rev. Lett. 121 (2018) 062501, https://doi.org/10.1103/PhysRevLett.121.062501.